Optimal Reference Strain Structure for Studying Dynamic Responses of Flexible Rockets

Natsuki Tsushima[1] and Weihua Su[2]
The University of Alabama, Tuscaloosa, AL, 35487-0280

Michael G. Wolf[3]
NASA Kennedy Space Center, Kennedy Space Center, FL 32899

Edwin D. Griffin[4] and Marie P. Dumoulin[5]
a.i. solutions, Inc., Cape Canaveral, FL 32920

Extended Abstract

Overview

In the proposed paper, the optimal design of reference strain structures (RSS) will be performed targeting for the accurate observation of the dynamic bending and torsion deformation of a flexible rocket. It will provide the detailed description of the finite-element (FE) model of a notional flexible rocket created in MSC.Patran. The RSS will be attached longitudinally along the side of the rocket and to track the deformation of the thin-walled structure under external loads. An integrated surrogate-based multi-objective optimization approach will be developed to find the optimal design of the RSS using the FE model. The Kriging method will be used to construct the surrogate model. For the data sampling and the performance evaluation, static/transient analyses will be performed with MSC.Natran/Patran. The multi-objective optimization will be solved with NSGA-II to minimize the difference between the strains of the launch vehicle and RSS. Finally, the performance of the optimal RSS will be evaluated by checking its strain-tracking capability in different numerical simulations of the flexible rocket.

I. Introduction

Altitude control of flexible rockets needs to take into account of their bending and torsion deformations during the launch. Actually, the observation of bending effects within launch vehicle structures currently exists within the aerospace industry; however, the cost and reliability of existing body bending sensors are continuing concerns. Fiber Optic Strain Sensors (FOSS) have been shown to provide useful strain data in aerospace structures such as rocket bodies and flexible

[1] Ph.D. Student (ntsushima@crimson.ua.edu), Department of Aerospace Engineering and Mechanics, Student Member AIAA.
[2] Assistant Professor (suw@eng.ua.edu), Department of Aerospace Engineering and Mechanics, Senior Member AIAA.
[3] Research Engineer (michael.wolf@nasa.gov).
[4] Research Engineer (edwin.d.griffin@nasa.gov).
[5] Project Manager (marie.p.dumoulin@nasa.gov).

aircraft wings. They may not only provide the ability to observe bending effects but also potentially control them. FOSS has demonstrated a reliable and predictable sensitivity to strain for mechanical structures; this capability gives rise to the potential use of FOSS coupled with various types of control systems. Therefore, FOSS systems must demonstrate that they can provide the accurate information necessary to replace existing body bending sensors in the launch vehicle industry.

In a previous study at the University of Alabama (UA) [1], a real-time beam bending solution was developed to obtain the instantaneous beam kinematics based on the measurement data from intermittent FOSS along the beam and a single inertia measurement unit (IMU). However, due to the difficulty in directly installing the FOSS on a rocket, a modular design of the reference strain structures has been considered, which are instrumented with FOSS and attached to the rocket. In order for the FOSS to accurately observe the bending strain of the rocket, the medium between the FOSS and rocket – the RSS – needs to be well designed. Therefore, the objective of the proposed paper is to first model a modular RSS with a full-size flexible rocket for further structural and flight studies. Based on the FE model, the RSS will be optimized with the intent of better observing the bending and torsion deformation of a flexible rocket. Finally, the feasibility of the optimal RSS will be proved by evaluating its performance of observing the strain of a flexible rocket.

II. Structural Analysis Model

This section describes the FE model of a notional flexible rocket with a modular RSS developed in MSC.Patran. It will be used for the structural analysis in the following sections.

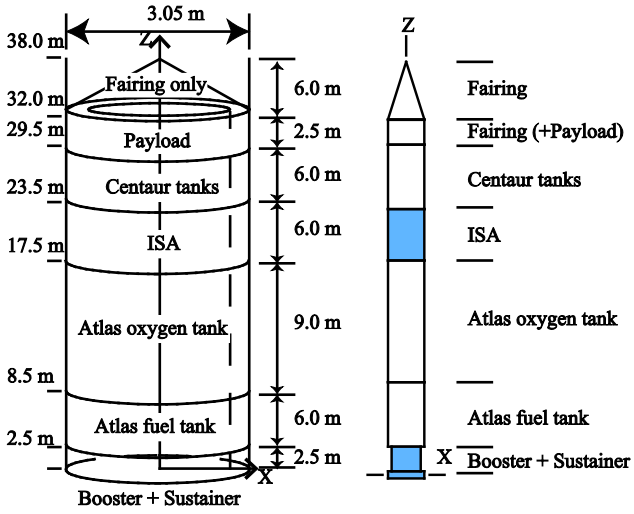

Figure 1. Flexible rocket model components.

A. Notional Flexible Rocket Model

A breakdown of the layers of the notional rocket is shown in Fig. 1. The geometrical and material properties are all obtained from Ref. [2] with other supplemental information from additional public resources. It consists of seven layers: a booster and sustainer, Atlas fuel tank, Atlas oxygen tank, interstage adapter (ISA), a cylindrical portion of a faring for the payload, and a conical nosecone of the fairing. The weight and bending rigidity distributions of the notional rocket with an empty tank configuration are shown in Fig. 2 [2]. The thickness of the cylindrical walls of different layers of the rocket is calculated based on the data as listed in Table 1. Poisson's ratio $\nu = 0.33$ is used for the materials of all layers. The cylindrical surface of the rocket is meshed using the CQUAD4 element in MSC.Patran, with 640 elements in the spanwise direction and 72

elements in the circumferential direction, respectively. In the following studies, internal tank pressures are applied on Atlas oxygen/fuel tanks and Centaur tank whose values are obtained from the lift-off test condition in Ref. [2].

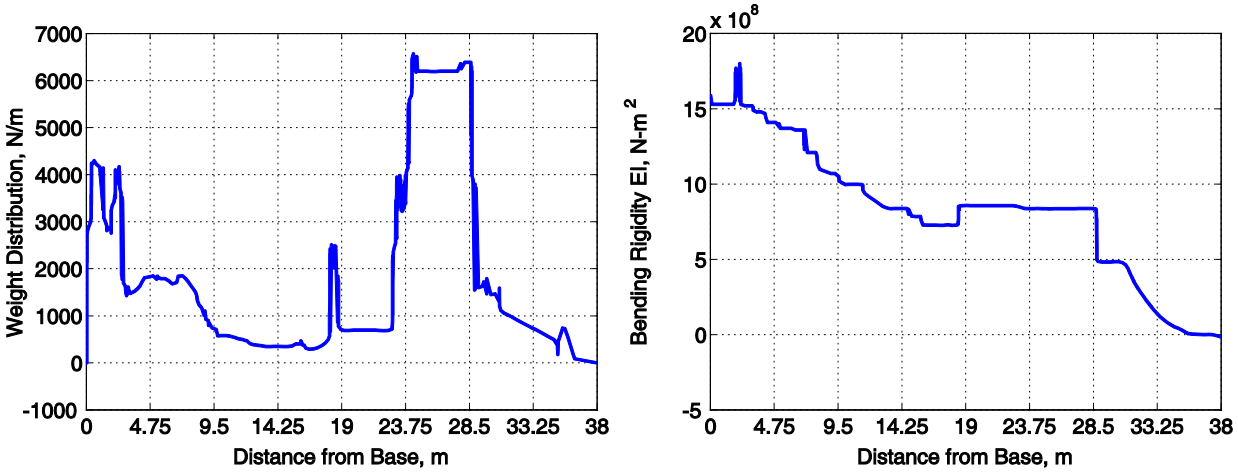

Figure 2. Weight and bending rigidity distributions of the notional rocket with empty tank.

Table 1. Wall thickness of each layer of the notional rocket.

Layer	Thickness, m
Fairing	0.015
Payload	0.005
Centaur tank	0.012
ISA	0.005
Atlas oxygen tank	0.005
Atlas fuel tank	0.005
Booster and sustainer	0.01

B. Reference Strain Structure Model

The FOSS will be instrumented on the RSS to collect its bending strain, which can be a good representative of the strain of the rocket if the RSS is well designed. In the current study, the RSS configuration is selected as a flat beam as shown in Fig. 3, while this design may be modified in the future. h = 3.18 mm is the beam thickness and b = 25.4 is the width. Rigid connections are used to link the rocket surface and the RSS. The axial spacing (l) of the links and the radial spacing (r) between the rocket and the RSS (see Fig. 3) may impact the strain-tracking performance of the RSS. Thus, the two spacing parameters will be considered as design variables in the following studies for the optimization. The material properties of the aluminum RSS beam are Young's modulus E = 70 GPa and Poisson's ratio ν = 0.33. The CQUAD4 element is also used to mesh the RSS beam, with 640 elements in the spanwise direction and 2 elements in the width direction, respectively. The finite element model consisting of both the rocket and RSS is shown in Fig. 4.

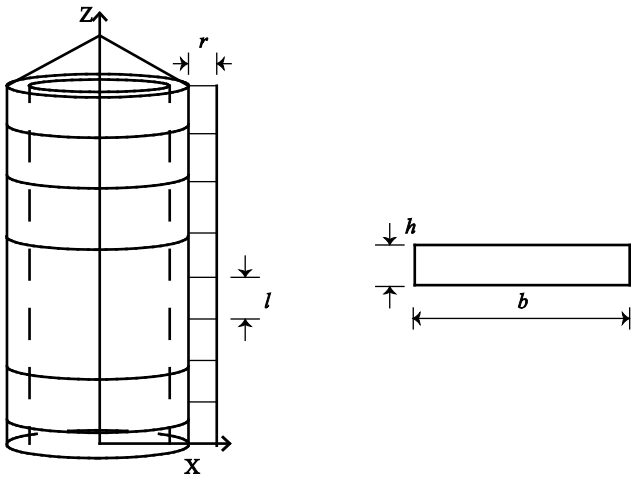

Figure 3. Dimension of RSS.

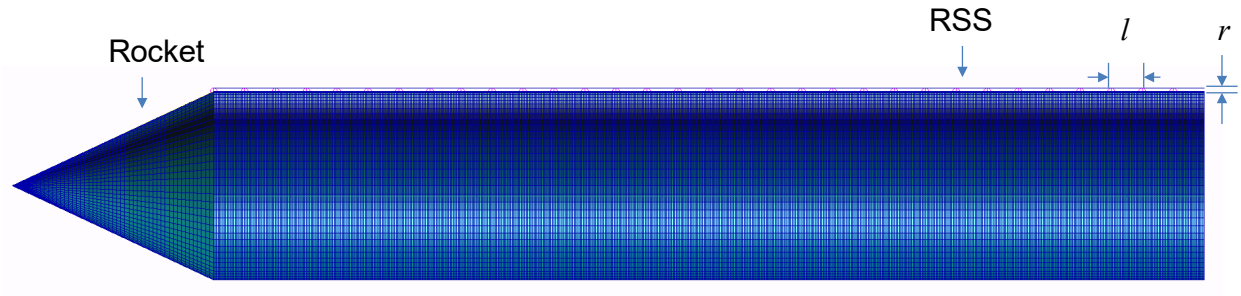

Figure 4. Finite element model of the notional rocket and RSS.

III. Design Optimization for the RSS-Rocket Linkage

As a preliminary study, the RSS design is chosen to be a flat beam with determined dimensions of width and thickness. As the axial and radial spacing of the links between the RSS and rocket impacts the strain-tracking performance of the RSS, a method to find the best spacing configuration so as to ensure a correct strain measurement from the FOSS is developed.

To find the optimal linkage spacing configuration, a surrogate-based optimization is performed, in which the surrogate model is constructed based on the FE simulation results from MSC.Nastran. In the process of generating the surrogate model, samples of the FE analysis results, which include the deformation and strain from both the rocket and RSS, are first obtained from MSC.Nastran. Among the different surrogate models, the Kriging method [3] is chosen because of its adaptive feature to the sampling (see Fig. 5). The surrogate model makes the total integrated optimization process fast because it provides an approximation of the objective function for the optimization with only a limited number of samples. For a global optimization, the genetic algorithm is used since it has a multi-objective optimization (MOO) capability as considered in the following discussion. The integrated optimization process is described in Fig. 5. The process consists of:

1. Develop the finite element model in MSC.Nastran/Patran.
2. Collect samples using the finite element model.
3. Construct the surrogate model based on the samples using Kriging.
4. Find the optimal spacing configuration with the Genetic Algorithm.
5. Perform static and transient analyses with the optimal setting and evaluate the strain tracking performance.

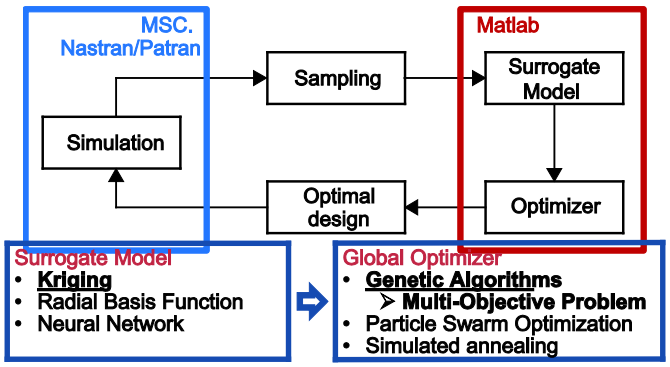

Figure 5. Integrated surrogate-based multi-objective optimization diagram.

A. Multi-Objective Optimization

The objective of the optimization is to minimize the strain difference between the rocket and the RSS beam, so that the rocket deformation is properly represented by the RSS deformation, which is further measured by the FOSS. As being discussed earlier, the performance of RSS is a function of the spacing of the linkage between the rocket and RSS. Therefore, the two objective functions of the optimization are the root mean square (RMS) axial strain (f_{axial}) difference between the RSS and the rocket, as well as the RMS transverse, or hoop (f_{hoop}), strain difference between the RSS and the rocket, which are given as

$$\min(f_{axial}(l,r) = \sqrt{\frac{1}{N}\sum_{n=1}^{N}\left(\varepsilon_{axial}^{rocket} - \varepsilon_{axial}^{RSS}\right)^2}) \tag{1}$$

and

$$\min(f_{hoop}(l,r) = \sqrt{\frac{1}{N}\sum_{n=1}^{N}\left(\varepsilon_{hoop}^{rocket} - \varepsilon_{hoop}^{RSS}\right)^2}) \tag{2}$$

where ε is the axial or hoop (transverse) strain on the notional rocket or the RSS. Actually, the transverse strain of the RSS is not a hoop strain, but the expression 'hoop' is used for convenience in this study. Several design constrains are considered in the study. For example, the two spacing parameters (l and r) are both limited in a range, given as

$$0.001 \le l \le 1 \tag{3}$$

$$0.001 \le r \le 0.1 \tag{4}$$

The last constraint is regarding the natural frequencies of the rocket and RSS. It is important to make sure that the natural frequencies of the rocket and RSS do not interfere each other so that the RSS is not excited by the vibration of the rocket. The constraint is shown as:

$$f_{nRocket} < f_{RSS} \tag{5}$$

where $f_{nRocket}$ are the natural frequencies of the notional rocket model and f_{RSS} are the natural frequencies of the RSS. The optimization problem is solved with the fast elitist nondominated sorting genetic algorithm (NSGA-II) [4].

B. Performance Evaluation

To evaluate the strain tracking performance of the RSS, the root mean square (RMS) difference (Δ_{rms}) and the error of the average strain between the rocket and RSS ($\bar{e}$) are calculated as follows:

$$\Delta_{rms} = \sqrt{\frac{1}{N}\sum_{n=1}^{N}\left(\varepsilon_{gage}^{rocket} - \varepsilon_{gage}^{RSS}\right)^2} \tag{6}$$

$$\varepsilon_{gage} = \varepsilon - \varepsilon_0 \tag{7}$$

$$\bar{e} = \left(\bar{\varepsilon}_{gage}^{Rocket} - \bar{\varepsilon}_{gage}^{RSS}\right) / \bar{\varepsilon}_{gage}^{Rocket} \times 100 \tag{8}$$

where ε_0 is pre-strain due to tank pressures, ε_t is the total strain on the rocket or RSS, and $\bar{\varepsilon}$ is an average strain. The RMS error is not used because there are singularities around the zero strain.

IV. Sample Numerical Results

In this section, sample analysis results with the RSS-rocket FE model are provided. The link spacing parameters will be optimized using the MOO approach discussed in the previous section.

A. Modal Analysis

The modal analysis is performed to compare the simulated natural frequencies of the notional rocket model with the experimental data in Ref. [2] as listed in Table 2. Note that the free-free boundary condition is used here. The natural frequency differences are less than 2 Hz, which are in the expected range for further control studies. In addition, as discussed in a previous section, the natural frequencies of the RSS should be out of the range of the frequencies of the rocket and the control system, which is defined from 0 to 500 Hz. Table 3 shows the natural frequencies of the RSS with the dependence on the axial spacing of the links. According to the table, it is preferred to constrain the axial spacing of the RSS-rocket links to be less than 0.1 m, so that the first three natural frequencies of the RSS do not interfere with those of the rocket.

Table 2. Natural frequencies of the bending modes of the notional rocket.

Bending mode	Direction	Simulated, Hz	Experiment, Hz
1st bending	Y-Z plane	3.78	2.59
	X-Z plane	3.78	2.60
2nd bending	Y-Z plane	7.10	6.49
	X-Z plane	7.10	6.52
3rd bending	Y-Z plane	11.01	9.82
	X-Z plane	11.01	10.01
4th bending	Y-Z plane	14.57	12.74
	X-Z plane	14.57	13.01
5th bending	Y-Z plane	18.58	17.98
	X-Z plane	18.58	17.90

Table 3. Natural frequencies of the RSS.

Axial spacing *l*, m	Bending mode	Frequency, Hz
0.1	1st bending	1475.5
	2nd bending	3592.9
	3rd bending	6852.4
0.5	1st bending	63.125
	2nd bending	174.91
	3rd bending	344.58
1	1st bending	16.173
	2nd bending	44.651
	3rd bending	87.668

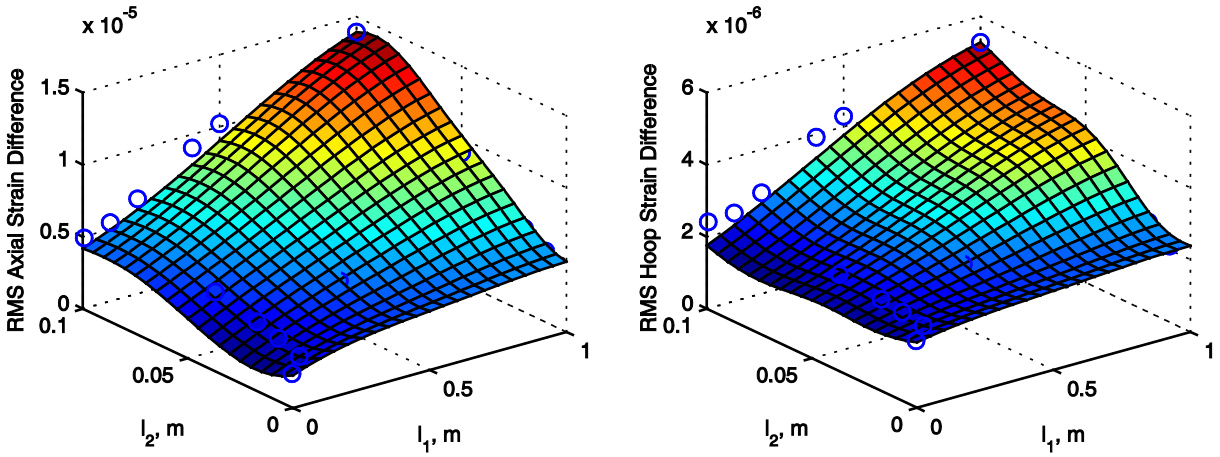

Figure 6. Surrogate model of RMS axial and hoop strain differences between rocket and RSS with static lateral loading.

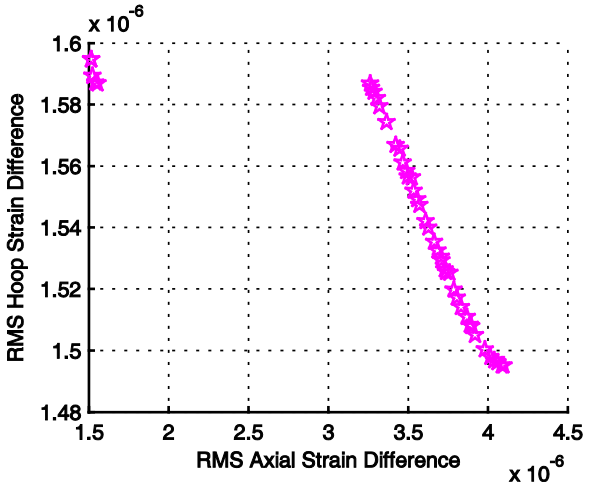

Figure 7. Pareto-optimal solutions with the static lateral loading.

B. Multi-Objective Optimization of Spacing Configuration

The integrated MOO is performed to find the optimal spacing of the connection between the rocket and the RSS. A 1 kN static lateral loading is applied at the top of rocket nosecone. The

Kriging-based surrogate model is firstly constructed to be used in the optimization process. 15 samples are obtained from the finite element analysis by MSC.Natran. The surrogate model predictions are given in Fig. 6, in which the samples are shown with blue circles. The Pareto-optimal (PO) solutions is shown in Fig. 7 . Based on the obtained PO solutions, the optimal axial spacing l is chosen to be 0.05 m and the optimal radial spacing r to be 0.01 m for a practical application by putting a priority to the axial strain tracking performance for future control studies.

C. Performance Evaluation with Static Loading

A static analysis is performed using the optimized model, where l = 0.05 m and r = 0.01 m. Tank pressures are 10.3×10^4 N/m^2 for Centaur tank, 40.5×10^4 N/m^2 for Atlas fuel tank, and 21.25×10^4 N/m^2 for Atlas oxygen tank. A constant 1 kN lateral force is applied at the top of the rocket. The resulting axial and hoop strains of the RSS and the rocket wall (where the RSS is attached) are compared in Fig. 8. The RMS axial strain difference is 2.2571×10^{-6} and the RMS hoop strain difference is 1.8153×10^{-6}. The errors of average axial and hoop strain are 0.43 % and 1.04 %, respectively. The strain jumps on the rocket due to the structural discontinuities are smoothed out by the RSS system, which is beneficial to the further control study.

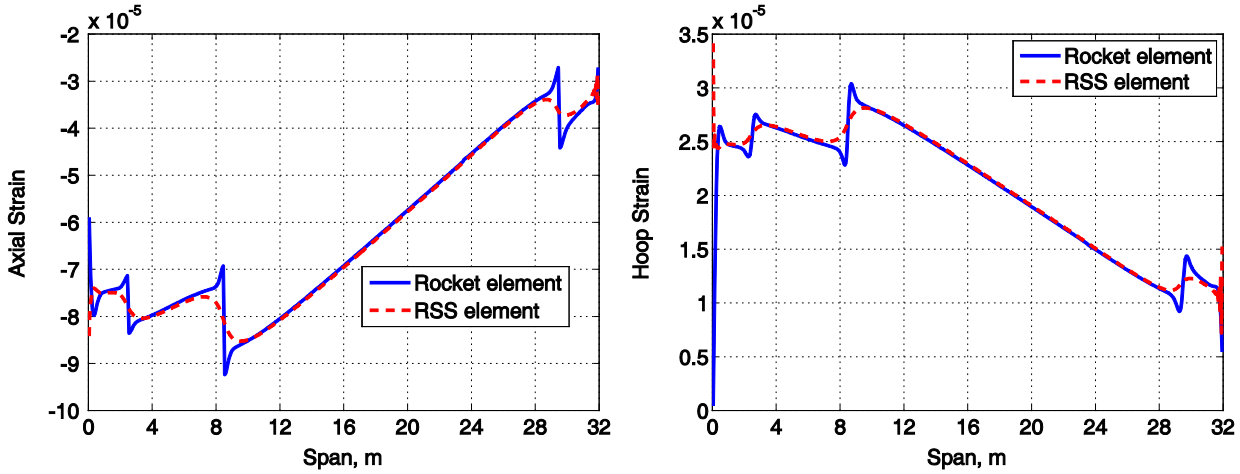

Figure 8. Axial and hoop strains on rocket and RSS with the designed spacing under the static lateral loading and tank pressures.

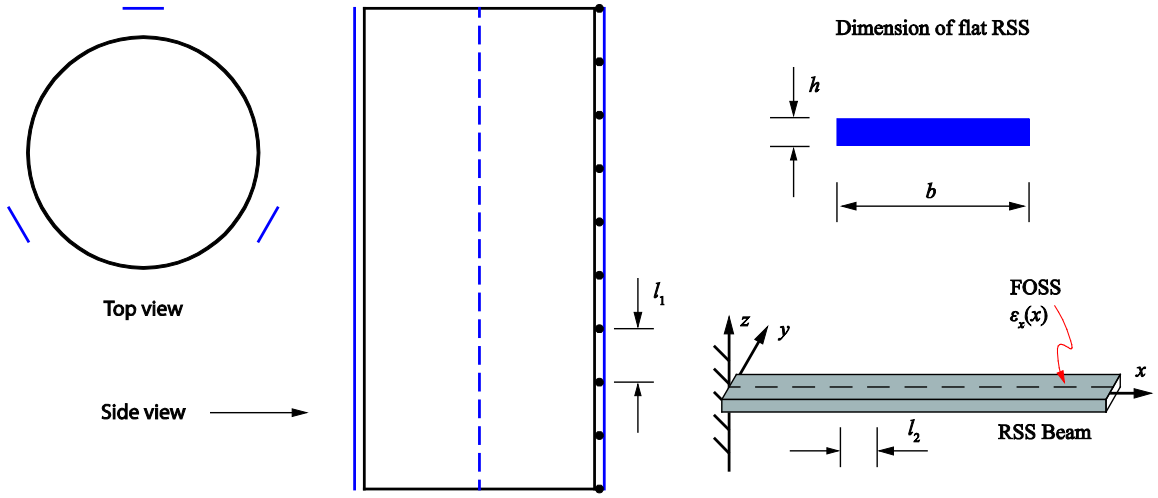

Figure 9. Three flat RSS beams attached to cylindrical surface of rocket.

V. Final Paper

In the final paper, a more comprehensive design optimization will be carried out with the two spacing (l and r) as well as the dimensions (thickness and width) of the RSS being the design variables. To allow for the collection of the rocket deformation in multiple axes, such as the complex bending-bending-torsion in the launch, it is desired to have three (or more) such flat RSS beams attached every 120 degrees around the rocket (see Fig. 9). Consequently, an "average" of the three RSS beams' strain measurements will be used to derive the corresponding strain and kinematics of the rocket center line. Lastly, the optimal design of the RSS will consider different load cases including both the static and transient loads of the rocket.

Acknowledgment

This work is supported by the NASA Launch Services Program Special Study.

References

1. Su, W., King, C., Clark, S., Griffin, E. D., Suhey, J. D., and Wolf, M. G. "Dynamic Beam Solutions for Real-Time Simulation and Control Development of Flexible Rockets," *57th AIAA/ASCE/AHS/ASC Structures, Structural Dynamics, and Materials Conference*. p. 1954.
2. Miller, R. P., and Gerus, T. F. "Experimental Lateral Bending Dynamics of the Atlas-Centaur-Surveyor Launch Vehicle." NASA TM-X-1937, 1969.
3. Krige, D. G. "A STATISTICAL APPROACH TO SOME BASIC MINE VALUATION PROBLEMS ON THE WITWATERSRAND," *Journal of the South African Institute of Mining and Metallurgy* Vol. 94, No. 3, 1994, pp. 95-111.
4. Deb, K., Pratap, A., Agarwal, S., and Meyarivan, T. "A fast and elitist multiobjective genetic algorithm: NSGA-II," *Evolutionary Computation, IEEE Transactions on* Vol. 6, No. 2, 2002, pp. 182-197.